Experimental Investigation of a Pulse Tube Refrigerator with Cold Compressor and Cold Phase Controller

B. Kim, J. Park and S. Jeong

Cryogenic Engineering Laboratory, Mechanical Engineering Dept.,
School of Mechanical and Aerospace Engineering,
Korea Advanced Institute of Science and Technology
291, Daehak-Ro, Yuseong-Gu, Daejon 34141, Rep. of Korea

ABSTRACT

Performance of the Stirling-type pulse tube refrigerator (SPTR) with cold compressor and cold phase controller is investigated. The cold compressor and the cold phase controller were submerged into liquid nitrogen, and maintained at constant temperature. The cold compressor produces PV work directly at cryogenic temperature and transmit its expansion work to the cold-end of the pulse tube refrigerator more effectively. The overall conversion efficiency is about 60% with 35 W of electric power input. The resonant frequency of the linear compressor is 47 Hz with the charging pressure of 2 MPa. First the experimental result exhibits no-load temperature of 45 K. From 2 m to 2.4 m length range of inertance tube, no-load temperature of CHX changes from 45 K to 35.1 K. In addition, the variation effect of the operating frequency is investigated. Depending on the length of the inertance tube, the optimum frequency corresponding to the lowest temperature of CHX changes. Small changes of the operating frequency results in significant increase of the no-load temperature. The performance of the SPTR is more sensitive to the geometry of the phase controller and operating frequency because of the cryogenic location of the phase controller.

INTRODUCTION

Stirling-type pulse tube refrigerators (SPTR) utilize oscillating pressure and mass flow to create cooling power directly. The efficiency of SPTR is generally maximum when the phase difference between pressure and mass flow becomes zero at the center of the regenerator [1]. To achieve this condition, an effective phase controller and an appropriate amount of PV work are necessary. In general, a linear compressor produces PV work at room temperature and the PV work is delivered to cold end of PTR. Passing through the regenerator, the PV work experiences significant amount of reduction. This phenomenon originates from pressure drop through the regenerator, and decrease of specific volume of working fluid, i.e. helium. It is obvious that the specific volume of working fluid is linearly correlated to temperature under the ideal gas assumption, and the low temperature of cold end of PTR leads to the decrease of specific volume and PV work. Consequently, delivering a large amount of PV work from the compressor to the cold end of the PTR is challenging and the lack of the amount of PV work results in low performance of the PTR. As a quick remedy, simple scaling-up of the geometrical size of PTR tends to bring a flow mixing problem and inhomogeneous flow in the pulse tube, resulting in poor performance of PTR [2]. On the other hand, a cold compressor

Cryocoolers 20, edited by S.D. Miller and R.G. Ross, Jr.

can generate PV work directly at cryogenic temperature, and delivers PV work to the cold end of the PTR effectively. Experimental setup, described in this paper, adopts a cold linear compressor and a cold phase controller (inertance tube-type). During the operation, both the cold linear compressor and the cold phase controller are maintained at 77 K. Several researchers adopted the cold phase controller previously in multi-stage PTR [3, 4]. They report that the phase between mass flow and pressure has been effectively shifted by maintaining the phase controller at low temperature. This cryogenic operating condition of the phase controller makes performance of the refrigerator to be highly sensitive to the geometry of phase controller. This paper specifically describes an experimental investigation on pulse tube refrigerator with a cold linear compressor and cold phase controller. The performance of the PTR with a different phase controller and operating frequency change is experimentally examined. Results of the detailed experiment and controller are presented.

EXPERIMENTAL SET UP

Experimental Apparatus

A schematic diagram of experimental setup is represented in Fig. 1. The lower part of SPTR is a linear compressor unit. A linear compressor used in the experiment is hermetically sealed and adopts a moving-magnet piston. A permanent magnet is radially attached to the piston. A piston is located at the middle of the coil, and keeps its position by a gas bearing. No mechanical support exists between piston and other component. Inner and outer yokes are installed under the top flange of the compressor unit. The inner and outer iron yokes create a magnetic field loop, and enlarge the electro-magnetic force on the piston with relatively small amount permanent magnet. The motor constant is 4.8 N/A at the given geometry of the compressor unit. An aftercooler, made of slitted copper, is connected at the top of the compressor unit, and provides thermal path between the working fluid and the heat sink. The oscillating pressure is measured by a dynamic pressure sensor, which is mounted in the aftercooler. The entire compressor unit is submerged into liquid nitrogen so that it is to generate PV work at isothermal condition of 77 K. A radiation shield, made of copper, is thermally anchored to liquid nitrogen to mitigate radiation heat transfer from the cryostat wall to PTR components. The regenerator,

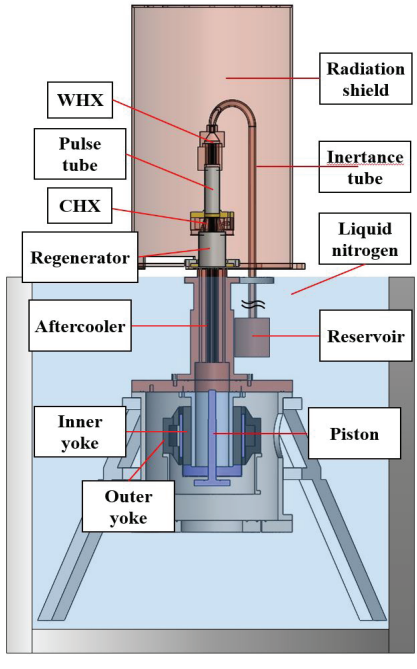

Figure 1. Schematic diagram of the Stirling-type pulse tube refrigerator

Table 1. Detailed information of the Stirling-type pulse tube refrigerator

Piston mass	260 g
Electric resistance	0.05 Ω
Electric inductance	1.9 mH
Motor constant	4.8 N/A
Regenerator	22.6 mm (O.D.), 40 mm (L), 0.3 mm (t)
	30 mm : #400 stainless steel mesh, porosity 0.65
	10 mm : 75 μm-diameter lead sphere, porosity 0.35
Pulse tube	12.7 mm (O.D.), 75 mm (L), 0.3 mm (t)
Phase controller	Inertance tube – 4.95 mm (I.D), 2 m (L)
	Reservoir – 500,000 mm3

cold end heat exchanger (CHX), pulse tube, warm end heat exchanger (WHX), and inertance tube are installed sequentially inside of the cryostat. A thermal strap connects the WHX and the radiation shield to reject heat from WHX. Temperatures of regenerator, cold end heat exchanger, and warm end heat exchanger is measured. All geometrical details of the PTR components are tabulated in Table 1. Some portion of the inertance tube and the entire reservoir are located outside of cryostat. Those parts are also submerged into liquid nitrogen, being maintained at isothermal condition.

Experimental Procedures

The SPTR, in this paper, adopts cold linear compressor and cold phase controller. A simple way of realizing such a condition is to submerge them into liquid nitrogen. The cryostat is first evacuated before cool down of the entire system. Then the entire system is charged with helium gas up to 2 MPa. After charging, liquid nitrogen is supplied into a bath where the compressor unit and the phase controller are located. Electric power is supplied to the linear compressor and the operating frequency is tuned to near the resonant frequency. The resonant frequency is specified by comparing the amplitude of current for each frequency at constant voltage. The amplitude of current becomes minimum at resonant frequency [5]. Fig. 2 shows the amplitude of current and operating frequency

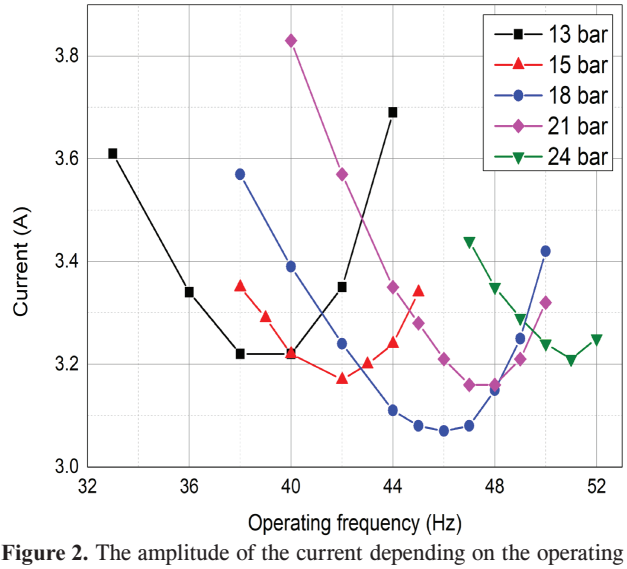

Figure 2. The amplitude of the current depending on the operating frequency

for various charging pressures. With a charging pressure of 20 bar, the resonant frequency is near 47 Hz. The temperature, dynamic pressure, supplying current, and voltage signals are collected by DAQ device.

EXPERIMENTAL RESULTS AND DISCUSSION

Dynamics of Linear Compressor and PV Work

During the experiment, the linear compressor operates at 77 K, receives electric power from the AC source, and generates PV work. Electric power input consumed by a linear compressor W_{Electric} is given by equation (1).

$$W_{Electric} = \frac{1}{2} V_0 I_0 cos\emptyset_{VI} \tag{1}$$

where V_o is the amplitude of voltage; I_O is the amplitude of current; $\emptyset_{VI}$ is the phase difference between voltage and current. $\emptyset_{VI}$ is determined from the electric characteristics of linear compressor. In addition, the displacement of piston is determined from following the force balance relationship. The simplified force balance and the voltage equation of linear compressor is given by Eq. (2) and Eq. (3).

$$m\ddot{x} + c\dot{x} + kx = -(P - P_b)A + \alpha_{motor} I \tag{2}$$

$$V = RI + L\frac{dI}{dt} + \alpha_{motor}\frac{dx}{dt} \tag{3}$$

where m is the mass of piston, c is the damping-coefficient, k is the spring constant, x is the piston displacement, P is the pressure of compression space, P_b is the pressure of bouncing volume, A is the area of the piston, R is the electrical resistance, L is the inductance of coil, V is the voltage, and I is the current. The force diagram of the piston can be made from the force balance equation by introducing the phases to x, P, P_b, and I. Fig. 3 shows the general force diagram of the piston (neglecting the pressure of bouncing volume). The displacement of piston is estimated from the relation between the current and pressure. Because mechanical linkage does not exist in the linear compressor, amplitude of the pressure and current with the phase between the pressure and the current determines the displacement of the piston. From the amplitude and phase of x and P the PV work produced at compression volume can be evaluated by Eq. (4).

$$W_{PV} = \pi f P_0 X_0 A \sin\emptyset_{xP} \tag{4}$$

where P_o is the amplitude of pressure oscillation; X_o is the amplitude piston displacement. The conversion efficiency of the linear compressor can be evaluated by taking the ratio of W_{Electric} and W_{PV} from the Eq. (1) and (2). The overall conversion efficiency of the linear compressor is 60% during the experiment.

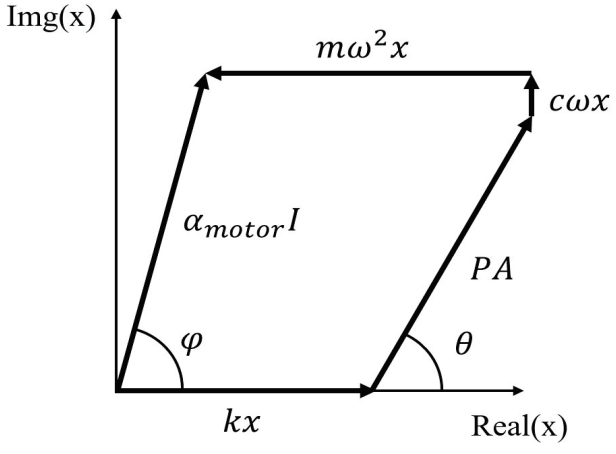

Figure 3. Force balance diagram of the piston

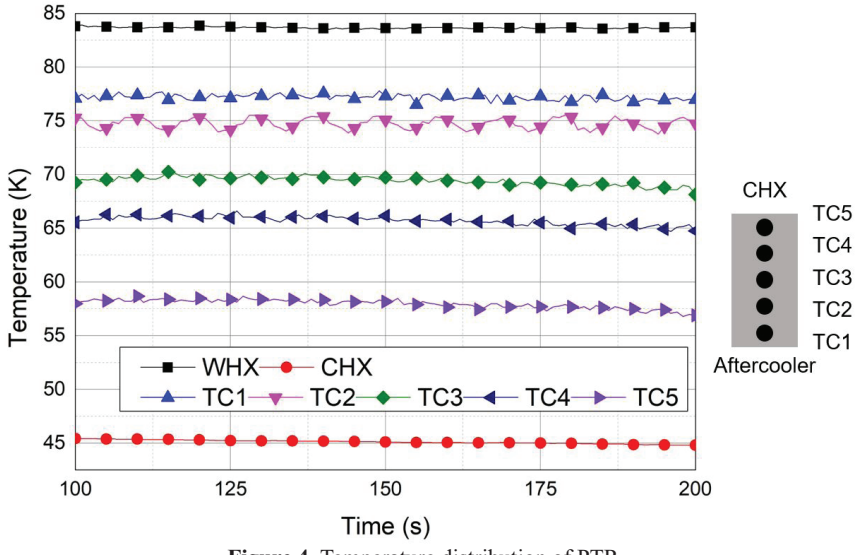

Figure 4. Temperature distribution of PTR

Experimental Result

After the PTR is cooled down to near 77 K, electric power is supplied to the linear compressor so that the PV work is generated. Fig. 4 shows the temperature distribution of the PTR components at steady state. TC1 to TC5 indicates the temperature of the surface of the regenerator. TC1 to TC5 is located on the surface of regenerator so that they are equally spaced between each other. TC5 is closest point to CHX. The operating frequency of the linear compressor is 47 Hz. The no-load temperature of CHX is about 45 K. Fig. 5 shows the oscillating signal of voltage, current, dynamic pressure at the after cooler, and dynamic pressure at the WHX. The phase between the current and the displacement of piston is about 90 , which implies the linear compressor is operating at resonant frequency. From the Eq. (1) and (4), the electric power input, PV work, and the conversion efficiency are calculated. The electric power is 36 W. The PV work is 20.6 W. The conversion efficiency is calculated as 57.2%.

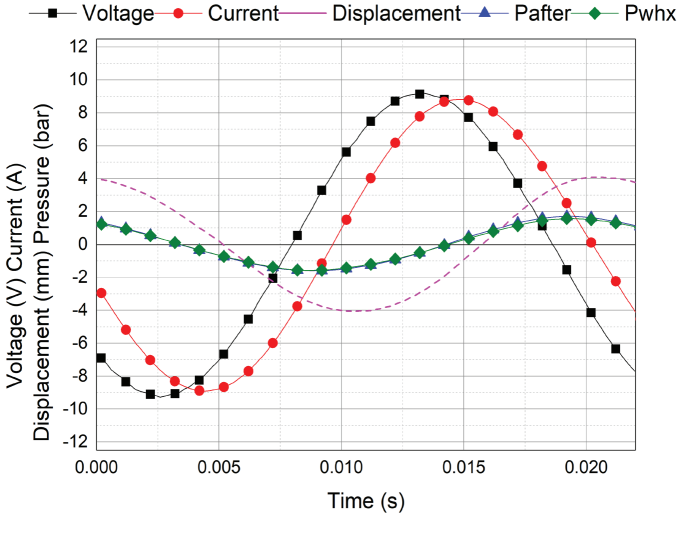

Figure 5. Oscillating voltage, current, pressure, and estimated displacement

Table 2. Temperature of CHX with the variation of inertance tube length

Length of inertance tube	2 m	2.2 m	2.4 m
Temperature of CHX	44.9 K	43 K	35.1 K

The effect of the inertance length is examined by comparing the no-load temperature of CHX. Variation of the inertance tube length is from 2 m to 2.4 m. Table 2 shows the no-load temperature dependence on the inertance tube length. The no-load temperature of CHX is significantly lowered at the inertance tube length of 2.4 m. It implies that the phase controller effectively makes phase shift between pressure and mass flow with an inertance tube length of 2.4 m. No-load temperature difference between inertance tube length of 2 m and that of 2.4 m is about 10 K. Similar to geometric effect of the inertance tube, the operating frequency of linear compressor also affects the performance of the PTR. Fig. 6 shows the no-load temperature of CHX depending on the operating frequency. L-2 m, L-2.2m, and L-2.4m indicate the length of the inertance tube respectively. The optimum frequency for the lowest no-load temperature changes with variation of the length of inertance tube. With the constant length of the inertance tube, small change of the operating frequency from the optimum frequency, 2 Hz, results in significant rise of the no-load temperature.

Discussion

Experimental results show that the variation of the length of the inertance tube and the operating frequency significantly influence the performance of the PTR. Even with the same electric input power to the linear compressor, the lowest temperature easily changes up to 10 K with slight variation from the optimum operating condition. This result implies that the cold phase controller is more sensitive than the common phase controller which is usually located at room temperature. The inertance tube can be modeled as equivalent circuit of a transmission line using an LRC circuit analogy. The complex impedance of inertance can be expressed as Eq. (5) to (8) [1].

$$Z = P/\dot{V} = \rho_0 P/\dot{m} = \rho_0 Z_m \tag{5}$$

$$r(D) = \left(\frac{2}{\pi}\right)\frac{32 f \dot{m}}{\pi^2 \rho_0 D^5} \tag{6}$$

$$l(D) = \frac{4}{\pi D^2} \tag{7}$$

$$c(D) = \frac{\pi D^2}{4\gamma R T_0} \tag{8}$$

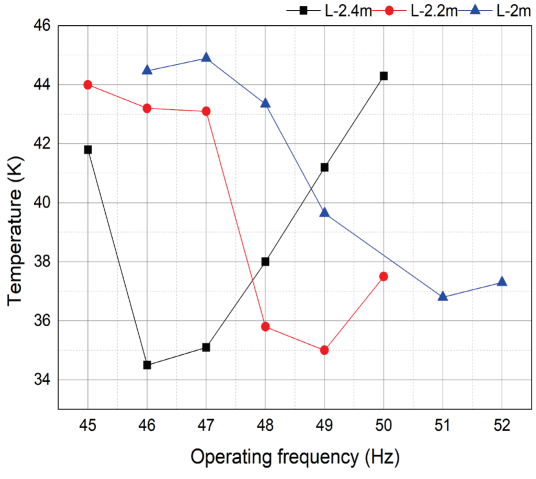

Figure 6. No-load temperature of CHX depending on the operating frequency

where r, l, and c represent resistance, inertance, and compliance per length, P is the pressure, $\dot{m}$ is the mass flow, D is the inside diameter of tube, f is the friction factor, γ is the ratio of specific heats. Above equations imply that each term is affected by the density of the fluid. The high sensitivity originates from the large inertia of the working gas as seen in the hydraulic impedance expression of inertance tube. This large inertia allows for a large phase shift, however, it makes the phase controller more sensitive. In order to mitigate the sensitiveness of cold inertance tube phase controller, a possible combination of active phase controller seems to be a good idea for further development.

CONCLUSION

The performance of the PTR with the cold linear compressor and the cold phase controller is experimentally investigated. The cold linear compressor exhibits 60 % of conversion efficiency, operating at 77 K. The resonant frequency of the linear compressor is around 47 Hz with the charging pressure of 2 MPa. Not only the fact that the current becomes minimum amplitude at resonant frequency for constant voltage but also the fact that relative phase between the current and the piston displacement is near 90^{o} supports that the linear compressor operates at resonant frequency. The no-load temperature of CHX is about 45 K with the inertance tube length of 2 m. The length change of the inertance tube has a significant impact on the no-load temperature of the CHX. The no-load temperature of CHX becomes lower from 44.9 K to 35.1 K with the change of length from 2 m to 2.4 m. The operating frequency, also, affects the performance of the PTR. Small changes in operating frequency from the optimum frequency causes a considerable increase of the no-load temperature of CHX. Experimental results imply that the cold phase controller is much more sensitive than a phase controller, that operates at room-temperature.

ACKNOWLEDGMENT

This research is supported by a grant from Space Core Technology Development Program of National Research Foundation of Korea (NRF-2013-042033) funded by Ministry of Science, ICT & Future Planning (MSIP).

REFERENCES

1. Radebaugh R, Lewis M, Luo E, Pfotenhauer JM, Nellis GF, Schunk LA., "Inertance Tube Optimization for Pulse Tube Refrigerators," *AIP Conference Proceedings*, Vol. 823, No. 1 (2006), pp. 59-67.
2. Willems DWJ, Backx V, Jonge AKD, "An Experimental Set Up for Large Scale Pulse Tube Refrigeration," *AIP Conference Proceedings*, Vol. 710, No. 1 (2004), pp. 1301-1308.
3. Qiu LM, Cao Q, Zhi XQ, Gan ZH, Yu YB, Liu Y, "A three-stage Stirling pulse tube cryocooler operating below the critical point of helium-4," *Cryogenics*, Vol. 51 (2011), pp. 609-12.
4. Zhi XQ, Han L, Dietrich M, Gan ZH, Qiu LM, Thummes G, "A three-stage Stirling pulse tube cryocooler reached 4.26K with He-4 working fluid," *Cryogenics*, Vol. 58 (2013), pp. 93-96.
5. Koh D-Y, Hong Y-J, Park S-J, Kim H-B, Lee K-S, "A study on the linear compressor characteristics of the Stirling cryocooler," *Cryogenics*, Vol. 42 (2002), pp. 427-432.